

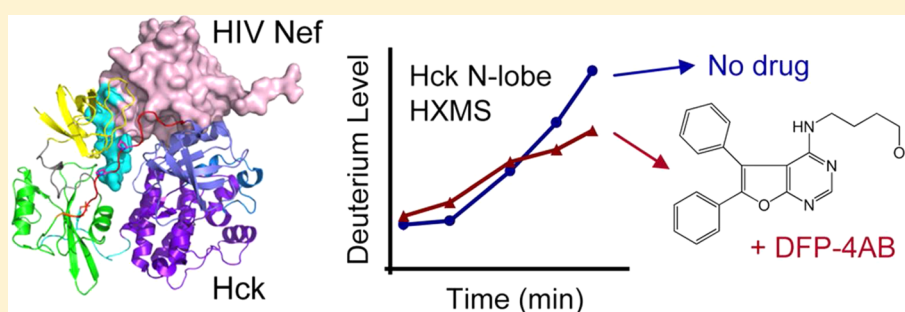
# Subtle Dynamic Changes Accompany Hck Activation by HIV-1 Nef and are Reversed by an Antiretroviral Kinase Inhibitor

Thomas E. Wales,<sup>†</sup> James M. Hochrein,<sup>†,§</sup> Christopher R. Morgan,<sup>†,||</sup> Lori A. Emert-Sedlak,<sup>‡</sup> Thomas E. Smithgall,<sup>‡</sup> and John R. Engen<sup>\*,†</sup>

<sup>†</sup>Department of Chemistry & Chemical Biology, Northeastern University, Boston, Massachusetts 02115, United States

<sup>‡</sup>Department of Microbiology and Molecular Genetics, University of Pittsburgh School of Medicine, Pittsburgh, Pennsylvania 15219, United States

## S Supporting Information



**ABSTRACT:** The HIV-1 virulence factor Nef interacts with the macrophage Src-family kinase Hck, resulting in constitutive kinase activation that contributes to viral replication and immune escape. Previous chemical library screens identified the diphenylfuranopyrimidine kinase inhibitor DFP-4AB, which selectively inhibits Nef-dependent Hck activity in biochemical assays and potently blocks HIV replication in vitro. In the present study, hydrogen exchange mass spectrometry (HX MS) was used to study conformational changes in downregulated Hck that result from Nef binding, as well as the impact of DFP-4AB on these changes. Remarkably, interaction with Nef induced only subtle changes in deuterium uptake by Hck, with the most significant changes in the N-lobe of the kinase domain adjacent to the docking site for Nef on the SH3 domain. No changes in hydrogen exchange were observed in the Hck SH2 domain or C-terminal tail, indicating that this regulatory interaction is unaffected by Nef binding. When HX MS was performed in the presence of DFP-4AB, the effect of Nef on Hck N-lobe dynamics was completely reversed. These results show that constitutive activation of Hck by HIV-1 Nef requires only modest changes to the conformational dynamics of the overall kinase structure. DFP-4AB reverses these effects, consistent with its activity against this Nef-induced signaling event in HIV-infected cells.

The hematopoietic cell kinase (Hck), a member of the c-Src protein-tyrosine kinase family, is expressed primarily in myeloid hematopoietic cells where it regulates immune receptor signaling, phagocytosis, as well as release of inflammatory cytokines.<sup>1</sup> Constitutive activation of Hck has been associated with several blood cancers, including acute and chronic myelogenous leukemias, and represents an important target for cancer drug discovery.<sup>2–5</sup> In addition, Hck is constitutively activated by HIV-1 Nef,<sup>6,7</sup> a virally encoded accessory protein essential for AIDS progression.<sup>8,9</sup> Nef-mediated activation of Hck in HIV-1 target cells contributes to enhanced viral replication<sup>10,11</sup> as well as MHC-1 down-regulation,<sup>12,13</sup> which is important for immune escape of HIV-infected cells. Several classes of small molecule inhibitors of Nef-dependent Hck activation have been discovered, and represent promising therapeutic leads for antiretroviral drug development.<sup>14–16</sup>

Hck, like other members of the Src-kinase family, is composed of an acylated N-terminal unique region, followed

by noncatalytic SH3 and SH2 domains, an SH2-kinase linker, a bilobed kinase domain, and a negative regulatory tail (Figure 1). X-ray crystal structures of downregulated Hck and c-Src show that intramolecular interactions of the regulatory domains allosterically control the kinase domain, holding it in the inactive state.<sup>17–20</sup> These interactions include binding of the SH3 domain to the SH2-kinase linker, which adopts a polyproline type II helix in the downregulated kinase, as well as interaction of the SH2 domain with the C-terminal tail. SH2–tail interaction requires phosphorylation of Tyr527 (all residue numbering as per the structure of human c-Src<sup>19</sup>) by the independent regulatory kinases, Csk and Chk.<sup>21</sup>

Hck and other Src-family kinases are activated as a result of protein–protein interactions that perturb the regulatory contacts between the SH3 domain and the linker or the SH2

**Received:** August 5, 2015

**Revised:** September 26, 2015

**Published:** October 6, 2015



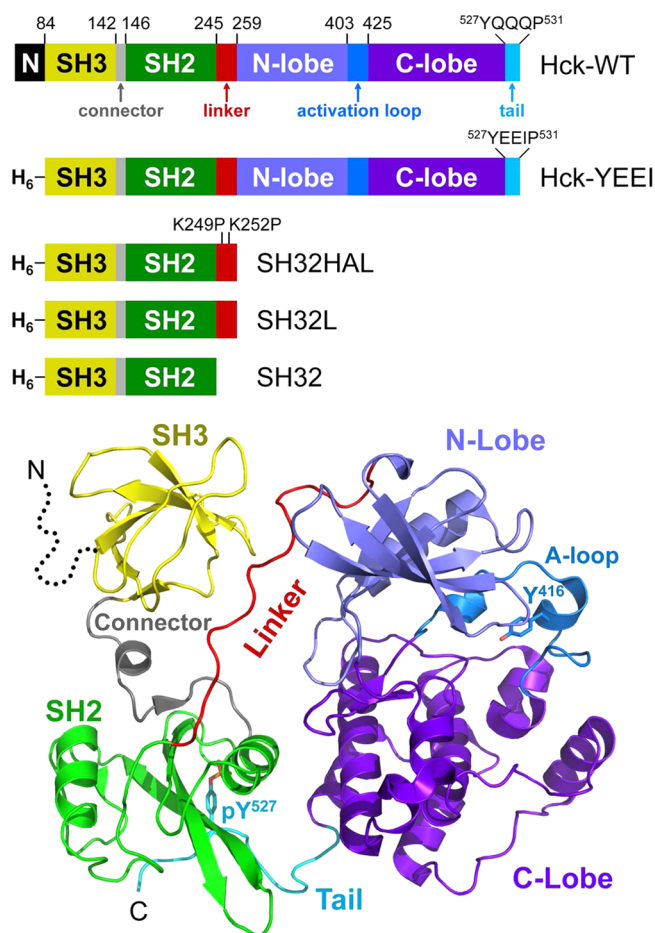


**Figure 1.** Structure of Hck and diagram of the recombinant proteins used in this study. Top panel: Hck consists of an N-terminal unique domain (N), regulatory SH3 and SH2 domains separated by a short connector, an SH2-kinase linker, and a bilobed kinase domain with small N-terminal and large C-terminal lobes. The activation loop contains the autophosphorylation site (Tyr416) while the wild-type regulatory tail contains the regulatory phosphotyrosine (pTyr527) followed by the sequence QQQP. In recombinant Hck-YEEI, the N-terminal region is replaced with a His-tag (H<sub>6</sub>) and the C-terminal tail sequence is modified to YEEIP. Smaller regulatory domain constructs include the SH3-SH2 unit plus a modified, high-affinity linker in which the two linker lysines shown are replaced with prolines (SH32HAL), the SH3-SH2 unit plus the wild-type linker (SH32L), and the SH3-SH2 unit without the linker (SH32). Bottom panel: Crystal structure of downregulated Hck-YEEI, with key structural elements colored as per the diagram at the top (PDB entry 1QCF).<sup>18</sup> The N-terminal unique domain is not present in the structure (dotted line).

domain and the tail. One of first and best-studied examples of displacement-based activation involves the interaction of Hck with the Nef protein of HIV-1.<sup>6,7</sup> The Nef protein has a conserved PxxPxR motif that engages the Hck SH3 domain, displacing the SH2-kinase linker and leading to kinase activation. Nef engages Hck with submicromolar affinity,<sup>22</sup> resulting in the formation of a stable, active Nef:Hck complex. In addition, cell-based experiments have indicated that Nef-dependent activation of Hck does not disrupt or require displacement of the SH2–tail interaction,<sup>23</sup> suggesting that Nef-bound Hck may represent a unique active form of the kinase amenable to inhibitor targeting. Support for this concept comes from recent drug discovery studies targeting the Nef:Hck complex, which identified a class of diphenylfurano-

pyrimidine compounds that preferentially inhibit Hck when bound to Nef as compared to Hck alone.<sup>10</sup> These compounds also inhibit Nef-dependent enhancement of HIV replication, suggesting that selective inhibition of the Nef–Hck signaling pathway may be of therapeutic benefit in HIV disease.<sup>10,11</sup>

While the structure of full-length, active Hck when bound to Nef is unknown, a recent crystal structure of Nef in complex with the SH3-SH2 regulatory unit of Hck (Hck32) provides important clues to the nature of the active Nef:Hck complex.<sup>24</sup> The individual Nef, SH2, and SH3 domain proteins that compose the dimeric Nef:Hck32 complex are virtually identical. However, the relative orientations of the SH2 domains in each of the two Nef:Hck32 complexes found in the crystal are quite different (Figure 2A). These distinct SH2 orientations result from structural differences in the two SH3–SH2 connector regions. Superposition of the crystal structure of each Nef:Hck32 complex onto the SH2 domain of the downregulated Hck structure<sup>17</sup> (Figure 2B,C) predicts SH3-linker displacement, supporting the SH3 domain displacement model of kinase activation described above. In downregulated Hck, SH2-kinase linker prolines P250 and P253 interact with SH3 domain residues Y90, W118, and Y136 at close range, with side-chain interaction distances ranging from 3.3 to 5.0 Å. While these SH3-linker interactions are displaced in both superposition models, the extent of displacement varies widely depending upon the Nef:Hck32 complex used to create each model. In the model based on Nef:Hck32 complex A, the linker prolines are displaced from the SH3 surface at distances ranging from 9.7 to 27.7 Å (Figure 2B). These distances are much greater in the model based on complex B, and range from 12.4 to 40 Å depending upon the SH3 surface residues involved (Figure 2C). These models raise important questions regarding the activation of Hck and other Src-family kinases by Nef: Which model more accurately represents the structure of the Nef-Hck complex? Does kinase activation by SH3 domain displacement require a major rearrangement of the regulatory domains, or is a more subtle change in position sufficient? What is the effect of antiretroviral inhibitors of Nef-induced Hck signaling<sup>10</sup> on the dynamic changes that accompany Hck activation by Nef?

In the present study, we used hydrogen exchange mass spectrometry (HX MS) to investigate the dynamic changes that accompany Hck activation by Nef in solution for the first time. We found that Nef binding to near-full-length, downregulated Hck did not result in global changes to backbone dynamics in the overall structure. Instead, only local perturbations were observed in the SH2-kinase linker and the small lobe of the kinase domain. These changes were completely reversed in the presence of a small molecule kinase inhibitor (diphenylfurano-pyrimidine 4-aminobutanol; DFP-4AB) previously shown to selectively inhibit Hck in the Nef-bound state. These findings show that Hck activation following Nef engagement correlates with remarkably small conformational changes as detectable by HX MS to the downregulated, assembled structure of Hck. More generally, our findings imply that activation of Src-family members and other multidomain kinases through partner protein recruitment may require only subtle perturbations to intramolecular regulatory interactions. Small molecules that stabilize or prevent these changes may be very effective at preventing kinases from adopting disease-specific states.

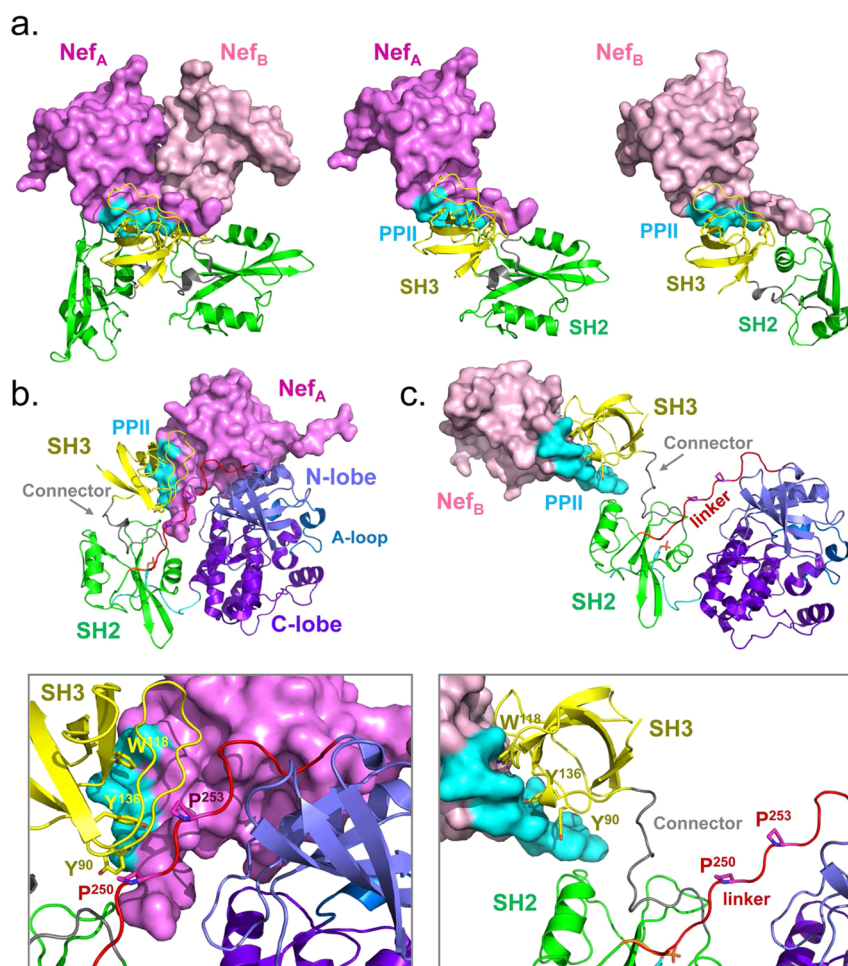


**Figure 2.** Molecular models of Hck in complex with HIV-1 Nef. (A) Crystal structure of Nef in complex with the Hck SH3-SH2 region<sup>24</sup> which forms a dimer of complexes (left). The Nef proteins (A and B) are rendered in different shades of pink, with the SH2 domains in green and the SH3 domains in yellow. The Nef PPII helix required for SH3 domain engagement is shown in cyan. The individual Nef:SH3-SH2 complexes are also shown separately (center and right) with the Nef proteins in the same orientation. Note that the SH2 domains are positioned quite differently between the two complexes. (B, C) Superposition models were produced by aligning each Nef:SH3-SH2 complex on the downregulated structure of Hck-YEEI via their SH2 domains. In the model based on the Nef<sub>A</sub> complex, the Nef PPII helix displaces the Hck SH2-kinase linker from the SH3 domain but remains in close proximity to the kinase domain N-lobe. The model based on the Nef<sub>B</sub> complex demonstrates much more dramatic displacement of the SH3 domain from the linker. The lower panels show key SH3 residues involved in Nef binding in each case (Tyr90, Trp118, and Tyr136) as well as SH2-kinase linker prolines 250 and 253 which engage SH3 in the absence of Nef.

## EXPERIMENTAL PROCEDURES

### Recombinant Hck and Nef Protein Expression.

Recombinant near full-length human Hck-YEEI was expressed in Sf9 insect cells and purified as described in detail elsewhere.<sup>10,25</sup> Hck-YEEI protein mass and tail phosphorylation were verified by mass spectrometry as described in ref 26. Recombinant Nef (B-clade “consensus” sequence) was expressed from the bacterial expression vector pET-14b with an N-terminal His-tag in *Escherichia coli* strain Rosetta 2(DE3)-pLysS (Stratagene) as described elsewhere.<sup>11</sup> Briefly, Nef expression was induced for 4 h with 1 mM IPTG at 37 °C. Following induction, cells were sonicated in binding buffer (20 mM Tris-HCl, 100 mM NaCl, 20 mM imidazole, 10% glycerol, 3 mM DTT, pH 8.3). Cell lysates were clarified by centrifugation and incubated with Ni-NTA beads at 4 °C for 1 h followed by elution in binding buffer supplemented with 200 mM imidazole. Fractions containing purified Nef protein were identified by electrospray ionization mass spectrometry, pooled, and dialyzed against buffer containing 20 mM Tris-

HCl, 100 mM NaCl, 3 mM DTT, pH 8.3. Proteins were divided into small aliquots and frozen at −80 °C until use.

**Analysis of Hck-YEEI Phosphorylation States.** For ATP preincubation studies, Hck-YEEI was incubated in the presence or absence of 10 mM MgCl<sub>2</sub> and 0.5 mM ATP for 60 min at 30 °C. Samples were injected onto a protein trap (MichromBio-Resources) and desalted for 3 min using 2% acetonitrile in water and a flow rate of 100 μL/min. After desalting, the acetonitrile concentration was stepped to 98% to elute the protein. The eluent from the HPLC was directed into a Waters/Micromass QToF2 for intact mass analysis. For phosphorylation site mapping, Hck-YEEI proteins were incubated with trypsin at 37 °C for 14 h. Tryptic peptides from 32 pmol of digested protein were separated on a C18 column (DionexPepMap 100, 3 μm, 100 Å, and 75 μm × 15 cm) using a 60 min gradient of acetonitrile and water at a flow rate of 3 μL/min followed by analysis on a Waters QToF2 mass analyzer. Sites of phosphorylation were confirmed using MS and MS/MS (see Figure S1).



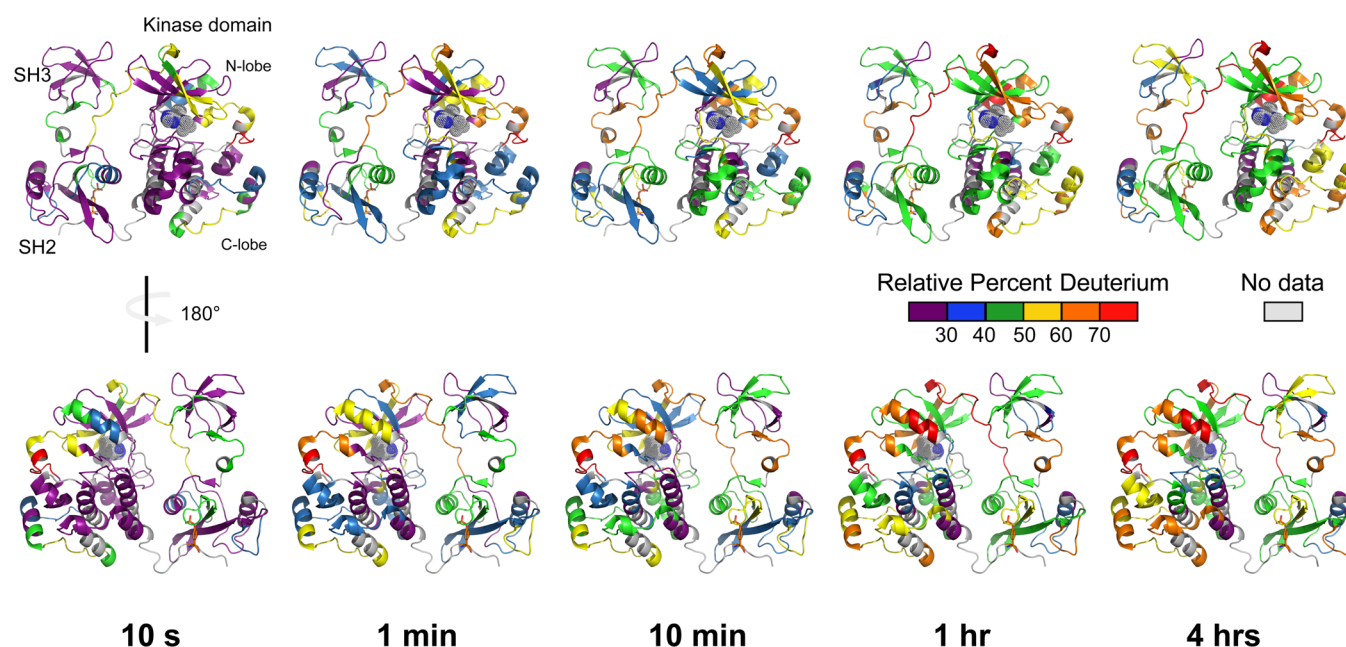


**Figure 3.** Deuterium incorporation into Hck-YEEI in the absence of ATP preincubation or Nef. Recombinant purified Hck-YEEI was exposed to deuterium over the time intervals shown. Following quenching of the deuterium uptake reaction, aliquots were digested with pepsin and deuterium uptake into individual peptides was determined by mass spectrometry (see [Experimental Procedures](#)). Relative percent deuterium incorporation into each peptide is mapped onto the crystal structure of downregulated Hck-YEEI ([Figure 1](#)) using a six-color scale corresponding to 10 s, 1 min, 10 min, 1 h, and 4 h of exposure to  $D_2O$  buffer. Regions of the protein without peptide data are shown in gray. Sequence and deuterium uptake data for each of the peptides used to create this figure are presented in [Table S1](#) and [Figure S4](#).

**Deuterium Labeling.** A stock solution of Hck-YEEI in Hck-YEEI dialysis buffer was prepared (4  $\mu M$  final). This solution was combined with an ATP or inhibitor (DFP-4AB) solution for a final volume of 70  $\mu L$ . In this 70  $\mu L$  volume, the Hck-YEEI concentration was 2.29  $\mu M$ , the ATP was 0.5 mM (with 10 mM  $MgCl_2$  present), or the DFP-4AB was 42.9  $\mu M$ . The solutions were incubated at 37  $^{\circ}C$  for 4 h before initiation of the deuterium labeling reaction or addition of Nef. In labeling reactions that included Nef, recombinant purified Nef (consensus B subtype<sup>27</sup>) was added to the Hck-YEEI reactions (plus ATP or DFP-4AB) to a final Nef concentration of 50  $\mu M$ . This mixture was incubated for an additional 30 min at 4  $^{\circ}C$  before initiation of the labeling reaction at 21  $^{\circ}C$ . Deuterium labeling was initiated by 15-fold dilution of reaction aliquots (each containing 16 pmoles of Hck-YEEI) into  $D_2O$  buffer containing 20 mM Tris-HCl, pH 8.3, 100 mM NaCl, and 3 mM DTT. In Nef binding experiments, the 15-fold dilution with deuterium labeling buffer resulted in concentrations of Hck-YEEI and Nef in the labeling reactions of 0.14  $\mu M$  and 3.13  $\mu M$ , respectively. Based on a  $K_D$  of 0.12  $\mu M$  for recombinant consensus Nef binding to the human Hck SH3 domain,<sup>22</sup> ~96% of the Hck-YEEI molecules were bound to Nef in the deuterium labeling solution. All calculations of percent bound were made as described in detail previously.<sup>28</sup> In the case of the DFP-4AB experiments, the labeling buffer contained 42.9  $\mu M$  DFP-4AB such that there was no dilution of the compound upon deuterium buffer addition. This concentration of inhibitor yields a  $K_i$  value of 8.4  $\mu M$  for the Nef:Hck-YEEI complex (derived from the Cheng–Prusoff equation and a DFP-4AB  $IC_{50}$  value of 16  $\mu M$ , an ATP assay concentration of 50  $\mu M$ , and the Hck-YEEI ATP  $K_m$  of 55.8  $\mu M$ <sup>10,26</sup>). Based on this  $K_i$ , we estimate that ~84% of Hck-YEEI in the labeling reaction was bound by DFP-4AB. At specific time points the labeling reaction was quenched by addition of an equal volume of

quench buffer (0.8 M guanidinium chloride and 0.8% formic acid, pH 2.5).

**Online Protein Digestion and Mass Analysis.** Quenched reactions were injected into a Waters nanoACQUITY with HDX technology for online pepsin digestion (15  $^{\circ}C$ ) and fast UPLC desalt and separation of peptic peptides (0.1  $^{\circ}C$ ).<sup>29</sup> Samples were injected onto a 2.1 mm  $\times$  50 mm stainless steel column that was packed with pepsin immobilized on POROS-20AL beads.<sup>30</sup> UPLC separation was achieved after the peptides were trapped and desalted on a VanGuard Pre-Column trap (2.1  $\times$  5 mm, Acquity UPLC BEH C18, 1.7  $\mu m$ ) for 3 min. Peptides were eluted from the trap using an 8–40% gradient of acetonitrile over 6 min at a flow rate of 40  $\mu L/min$  and were separated using an Acquity UPLC BEH C18 1.7  $\mu m$  1.0  $\times$  100 mm column. Peptides that were produced from the enzymatic cleavage of the unlabeled protein were identified from the triplicate analysis of undeuterated control samples using a combination of Waters MS<sup>E</sup> technology on a Waters QTOF Premier and ProteinLynx Global Server (PLGS) searches of a customized database.

All mass spectra were acquired using a Waters QTOF Premier mass spectrometer. Each deuterium labeling experiment was performed in duplicate. The error of determining the average deuterium incorporation for each peptide was at or below  $\pm 0.2$  Da. Mass spectra were processed with software supplied from Waters, combined with HX-Express.<sup>31</sup> Relative deuterium levels for each peptide were calculated by subtracting the average mass of the undeuterated control sample from that of the deuterium-labeled sample for isotopic distributions corresponding to the +1, +2, or +3 charge state of each peptide. The data were not corrected for back exchange and are therefore reported as relative.<sup>32</sup>

## RESULTS

**Hck-YEEI as a Model for Downregulated Hck.** Meaningful analysis of the impact of Nef binding on the conformational dynamics of Hck required purified Hck protein that adopts the downregulated state. Therefore, we used a form of Hck in which the wild-type C-terminal tail sequence that engages the SH2 domain (pTyr-Gln-Gln-Gln) is replaced with pTyr-Glu-Glu-Ile.<sup>33</sup> This simple modification promotes tail phosphorylation in the absence of Csk, enabling purification of the singly phosphorylated, downregulated conformation. X-ray crystallography has shown that this form of Hck, known as Hck-YEEI, adopts the same downregulated structure as wild-type Hck that is coexpressed with Csk<sup>17,18</sup> and is readily activated by recombinant purified Nef *in vitro*<sup>25</sup> and in cell-based systems.<sup>23</sup>

Hck-YEEI was expressed in Sf9 insect cells and purified to homogeneity as described previously.<sup>25</sup> Intact mass analysis showed that Hck-YEEI was singly phosphorylated, while incubation with ATP resulted in phosphorylation at a second site (Figure S1A). Tryptic peptide mapping confirmed single phosphorylation at the C-terminal tail (Tyr527) in the absence of ATP and additional phosphorylation in the kinase domain activation loop (Tyr416) after ATP incubation (Figure S1B), as we reported previously for an identical preparation of Hck-YEEI.<sup>26</sup>

**HX MS of Hck-YEEI Alone.** HX MS was performed first on Hck-YEEI in the absence of Nef or ATP to provide a baseline of comparison for the effect of Nef in terms of regional deuterium uptake. Overall, peptic peptides were obtained that covered 86% of the overall Hck-YEEI sequence. A peptide coverage map is provided in Figure S2 and details of the peptide ions that were monitored are shown in Supplementary Table S1. Example mass spectra for some peptides are shown in Figure S3. Overall, ~2/3 of the backbone amide hydrogens underwent less than 30% exchange within 10 s, consistent with a folded, dynamically stable protein, while the other ~1/3 of the backbone amide hydrogens were rapidly deuterated (Figure 3). The core of the structure formed by the interface of the SH2 and kinase domains reached only 50% exchange after 4 h of labeling, indicating that this region is very stable. In contrast, a few regions did show more rapid exchange, including the SH2-kinase linker which has a key regulatory role. Specific changes in peptides derived from this and other regions important to kinase regulation are described in more detail below.

**Engagement of the SH3-SH2 Regulatory Domains.** Previous studies from our group have established that the isolated recombinant Hck SH3 domain naturally displays a cooperative unfolding event with an average unfolding half-life close to 17 min (for a recent review, see Engen et al.<sup>34</sup>). The SH3 “unfolding half-life” increases following engagement with peptide ligands, both in *trans* and in *cis*.<sup>34</sup> Subsequent work showed that a single peptide of the Hck SH3 domain, encompassing residues 119–136, is central to the cooperative unfolding event that is responsive to ligand binding. The kinetics of deuterium uptake by this SH3 peptide therefore serves as a useful “reporter” for SH3 engagement, both in the isolated SH3 domain as well as in larger protein constructs. To determine whether the SH3 domain was engaged with the SH2-kinase linker in the context of Hck-YEEI, we compared the kinetics of deuterium uptake by the SH3 reporter peptide in the context of the following recombinant purified Hck proteins

(Figure 1): the SH3-SH2 (SH32) unit, SH3-SH2 plus the wild-type linker (SH32L), SH3-SH2 plus a modified high-affinity linker (SH32HAL) sequence previously shown to enhance interaction with SH3,<sup>35</sup> and Hck-YEEI itself. As shown in Figure 4A, the rate and extent of deuterium incorporation into

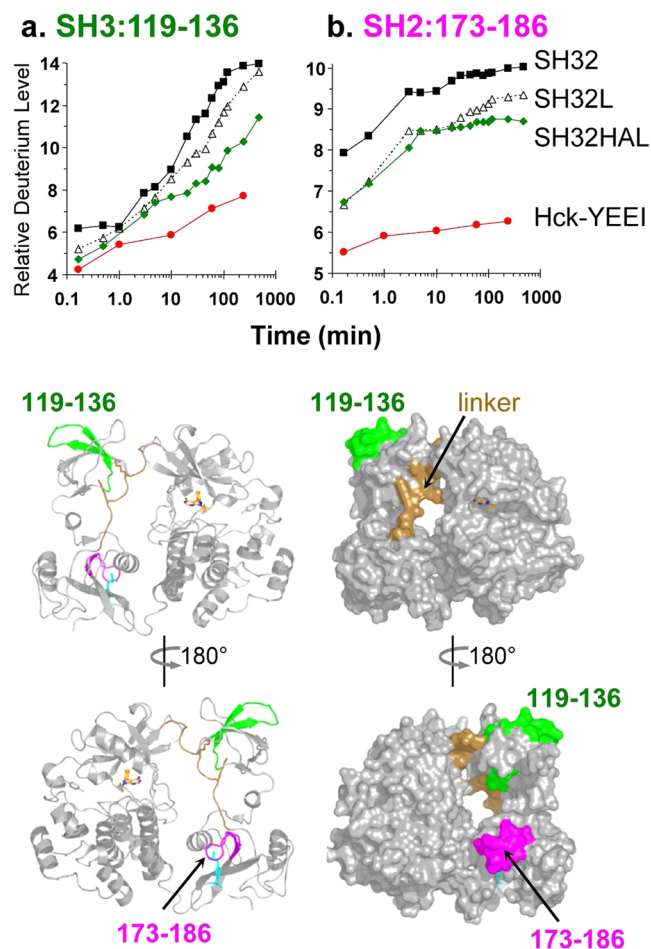


**Figure 4.** Deuterium incorporation by the SH3 and SH2 domains of Hck-YEEI as well as shorter proteins derived from the regulatory region. Deuterium uptake curves are shown for peptic peptides derived from the SH3 domain (119–136, panel a, left) and the SH2 domain (173–186, panel b, right) for the SH32 (black squares), SH32L (open triangles), SH32HAL (green diamonds), and Hck-YEEI (red circles) proteins (see Figure 1). Amino acid sequences of each peptide are presented in Table S1. The location of each peptide is illustrated on ribbon and space-filling models of Hck-YEEI below the graphs; the models have been oriented to show both the “front” and “back” of Hck-YEEI.

the SH3 reporter peptide was reduced to the greatest extent in Hck-YEEI, consistent with strong SH3-linker engagement in the context of the near-full-length, downregulated state. Deuterium incorporation in another peptide (residues 101–108) in the SH3 domain known to show reduced deuterium uptake upon ligand binding was also lower in the downregulated state (data not shown).

We also previously identified an SH2 domain reporter peptide that demonstrates reduced deuterium uptake when the SH2 is bound to a ligand. This peptide corresponds to SH2 residues 173–186 and encompasses a portion of the pocket responsible for engaging the phosphorylated C-terminal tail tyrosine important for Hck downregulation.<sup>36</sup> Deuterium

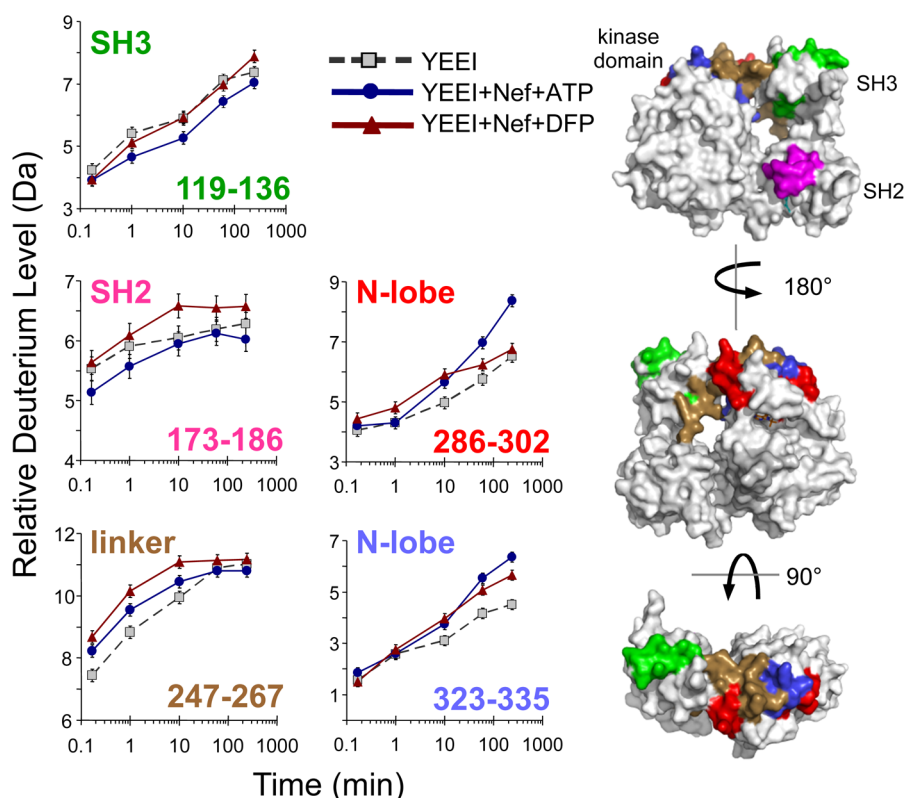


**Figure 5.** Regional changes in Hck-YEEI deuterium incorporation in response to HIV-1 Nef binding in the presence of ATP or the antiretroviral kinase inhibitor, DFP-4AB. Deuterium incorporation plots are shown for selected peptic peptides derived from Hck-YEEI alone (gray squares), Hck-YEEI plus Nef and ATP (blue circles), and Hck-YEEI plus Nef and DFP-4AB (red triangles). Peptides are derived from the SH3 (119–136) and SH2 (173–186) domains, the SH2-kinase linker (247–267 and 286–302), and the N-lobe of the kinase domain (323–335). The sequences of these peptides are listed in Table S1, and all deuterium incorporation graphs are shown in Figure S6. The sequence numbers of each peptide are color-coded and mapped onto space-filling models of Hck-YEEI (right). The standard error of each deuterium incorporation measurement is  $\pm 0.2$  Da as indicated by the error bars for each time point.

uptake by the SH2 reporter peptide is presented in Figure 4B for the same four Hck proteins described above. As observed with the SH3 domain, deuterium incorporation by the SH2 domain is also dramatically reduced in the context of Hck-YEEI compared to the other three proteins, all of which lack the kinase domain and tail. This observation suggests that the SH2 domain is engaged with the tyrosine-phosphorylated tail as required for maintenance of the downregulated state. Note that the extent of deuterium uptake by the SH32L and SH32HAL proteins is lower than that observed for the SH32 construct, even though the rate of uptake is very similar. This observation is consistent with previously reported stabilizing contacts<sup>37</sup> between the N-terminal end of the linker and the SH2 domain<sup>38</sup> that are not present in the SH32 protein.

In addition to the data provided by the SH3 and SH2 reporter peptides, analysis of peptides derived from the kinase domain of Hck-YEEI provided insight. A wide range of deuterium uptake rates and levels were observed, supporting diverse conformational flexibility (see Figure 3 and Figures S4 and S6). Peptides corresponding to the activation segment of Hck-YEEI (408–424; red peptide in Figure S2) showed very rapid deuterium uptake, indicating that this region of the kinase domain is highly dynamic and solvent-exposed. This result was not unexpected as the first crystal structure of naturally downregulated Hck<sup>18</sup> lacked electron density in the activation loop region. Only after incorporating an inactivating mutation in the kinase domain and a small molecule inhibitor at the ATP-binding site<sup>17</sup> was the activation loop stabilized enough to

define the electron density. In contrast to the activation loop and the N-lobe, several peptides derived from the C-lobe showed very slow deuterium uptake kinetics. This observation is consistent with the structure of the C-lobe, which consists of a packed bundle of  $\alpha$ -helices that protects backbone amide hydrogens from deuterium exchange.

**Activation and Inhibition Selectively Alter Hck Dynamics.** We next investigated the effect of autophosphorylation on the regional dynamics of Hck-YEEI in the absence of Nef. To accomplish this, Hck-YEEI was incubated with ATP and  $Mg^{2+}$  under conditions that result in stoichiometric phosphorylation of the activation loop on Tyr416.<sup>26</sup> The location and extent of Tyr416 phosphorylation was confirmed by mass spectrometry of tryptic digests (Figure S1B and data not shown; see also Moroco et al.<sup>26</sup>). HX MS was then performed on the autophosphorylated form and the results compared with those from the unphosphorylated form. Only small and few changes were observed in deuterium uptake for peptides derived from most of the Hck-YEEI protein (see Figure S4 for deuterium uptake curves for all peptides). In particular, neither the SH3 nor the SH2 domain reporter peptides showed a difference in exchange as a function of kinase domain autophosphorylation, indicating that activation loop phosphorylation per se does not cause allosteric changes in the interaction of these regulatory domains with their respective internal ligands (see also Figure S5).

As a counterpoint to ATP preincubation, we also performed HX MS on Hck-YEEI in the presence of the small molecule



inhibitor, DFP-4AB. This compound was discovered in a high-throughput screen for selective inhibitors of the Nef-Hck complex and displays Nef-dependent antiretroviral activity.<sup>10</sup> The DFP-4AB furanopyrimidine pharmacophore is predicted to bind to the Hck active site, making contacts with the hinge region connecting the N- and C-lobes of the kinase domain. This prediction is based on similar hinge region interactions observed in the X-ray crystal structure of a closely related inhibitor bound to the active site of the Src-family member, Lck.<sup>39</sup> Hck-YEEI was incubated with DFP-4AB at 42.9  $\mu$ M, which is in excess of the IC<sub>50</sub> value previously reported for Hck-YEEI,<sup>10</sup> followed by HX MS analysis. Rates of deuterium uptake were determined at the peptide level, and results were compared to those obtained with the unbound form (Figure S5). As was the case for phosphorylated Hck-YEEI above, minor changes in deuterium uptake were observed at the interface between the small and large lobes of the kinase domain, with no changes elsewhere in the protein. Slower uptake was observed in the hinge region at the first time point sampled (10 s), consistent with furanopyrimidine pharmacophore interaction with this region (Figure S5). DFP-4AB binding also resulted in a slight increase in deuterium incorporation for the  $\alpha$ -helix located below the activation segment (Figure S5), suggesting additional allosteric changes in the region adjacent to the presumed binding site for this compound.

**Unexpectedly Modest Changes in Global Protein Dynamics.** Molecular models based on the recent X-ray crystal structure of HIV-1 Nef in complex with the Hck SH3-SH2 region<sup>24</sup> support the SH3 domain displacement mechanism of kinase activation (Figure 2). However, the extent of SH3 domain displacement required for the activating event, as well as the effect of Nef binding on other regulatory interactions present in the downregulated state (e.g., SH2-phosphotail interaction), remain unknown. To address this issue, we performed HX MS on Hck-YEEI in the presence of recombinant purified Nef (B-clade “consensus” sequence), which has been previously shown to bind to the Hck SH3 domain in the submicromolar range and induce robust activation of recombinant Hck-YEEI *in vitro*.<sup>22</sup> Nef was added in sufficient molar excess to ensure that more than 95% of Hck-YEEI was in the bound state. In addition, the experiment was performed in the presence of ATP so that the resulting Nef-Hck complex attains the active state. The protein mixture was then subjected to deuterium exchange, followed by MS analysis of the peptic peptides derived from Hck-YEEI. Deuterium uptake curves for all of the Hck-YEEI peptides followed in the exchange reaction are shown in Figure S6.

Very few Hck-YEEI peptides showed significant changes in hydrogen exchange upon Nef binding, defined as a difference in deuterium incorporation that is greater than 0.5 Da,<sup>40</sup> relative to downregulated Hck-YEEI. The SH3 domain reporter peptide (119–136) showed no change following Nef binding (Figure 5). This result is consistent with the displacement of the SH3 domain from the SH2-kinase linker by Nef; because both Nef and the linker compete for the same SH3 binding site, no net change in SH3 reporter peptide exchange was anticipated. Peptide 247–267, on the other hand, shows an increase in deuterium exchange in the presence of Nef. This peptide includes a significant portion of the SH2-kinase linker, as well as the N-terminal portion of the kinase domain N-lobe. Thus, Nef binding may alter the position of the linker in a manner consistent with kinase domain activation. The SH2

domain reporter peptide (173–186) did not show a change in deuterium uptake in response to Nef binding. This result provides the first direct biophysical evidence that Nef binding does not affect SH2–tail interaction and supports previous cell-based studies showing that Nef-induced Hck activation occurs without tail dephosphorylation or release from the SH2 domain.<sup>23</sup>

Two peptides derived from the kinase domain showed significant increases in deuterium incorporation in the presence of Nef. These peptides include amino acids 286–302 and 323–335 and map to the portion of the N-lobe that is comprised of  $\beta$ -sheet and flanks the  $\alpha$ C-helix (Figure 5). Both peptides pack against the C-terminal end of the SH2-kinase linker in the downregulated structure, suggesting that Nef binding to SH3 and subsequent release of the linker may result in allosteric increases in the flexibility of these kinase domain peptides as well. Interestingly, the 286–302 peptide includes the highly conserved residue Lys295, which forms a stabilizing salt bridge with Glu310 in the active conformation based on comparison with the active form of the closely related Lck kinase domain.<sup>41</sup> In contrast, incubation of Hck-YEEI with ATP in the absence of Nef did not influence deuterium uptake into this peptide (Figure S4). Thus, Nef binding may selectively enhance the dynamics of this region of the kinase domain, and facilitate Lys–Glu interaction as part of a unique Nef-dependent activation mechanism. Note that two peptides derived from the N-lobe  $\alpha$ C helix, which encompasses Glu310 and undergoes inward rotation during kinase activation, showed barely significant increases in deuterium exchange across the time scale examined (see Figure S6). This observation suggests that the  $\alpha$ C helix is very dynamic, irrespective of the presence of Nef.

**DFP-4AB Reverses Nef-Induced Changes.** In a final experiment, we performed HX MS on Hck-YEEI in the presence of both Nef and the small molecule inhibitor, DFP-4AB. As described above, this compound shows higher inhibitory potency for Hck-YEEI when bound to Nef versus Hck-YEEI alone and also displays Nef-dependent antiretroviral activity in cells infected with HIV expressing a broad range of Nef alleles.<sup>10,11</sup> The Hck-YEEI/Nef protein mixture was equilibrated with DFP-4AB at 5-times the calculated K<sub>i</sub> based on the IC<sub>50</sub> value originally reported for inhibition of this complex *in vitro* (see Experimental Procedures).<sup>10</sup> The reaction was then subjected to deuterium exchange, followed by MS analysis of the Hck-YEEI peptides as before. All of the Hck-YEEI peptides monitored in the exchange reaction in the presence of Nef and DFP-4AB are shown in Figure S6, and a summary of the changes is shown in Figure S7. Change was observed in the kinase domain N-lobe peptide, 286–302, which encompasses Lys295 and is selectively sensitive to Nef in terms of deuterium uptake as described above. In the presence of DFP-4AB, however, this peptide displayed deuterium uptake kinetics very similar to those observed in the absence of Nef (Figure 5). This observation suggests that selective inhibition of the Nef:Hck-YEEI complex by this compound results in part from reversal of the allosteric enhancement of Lys295 mobility observed in the presence of Nef.

## DISCUSSION

In this study, we report regional changes in dynamics for the Src-family kinase, Hck, in various states including the assembled, downregulated state; following activation by preincubation with ATP; upon interaction with the SH3-

binding protein, HIV-1 Nef; and in the presence of a selective inhibitor (DFP-4AB) previously shown to alter Nef-induced Hck activation. On the basis of comparisons of regional exchange into smaller Hck proteins consisting of only the regulatory domains, we show that the SH3 domain is engaged with the linker and that the tail remains bound to the SH2 domain in solution, consistent with X-ray crystal structures for the downregulated, assembled state of Hck.<sup>17,18</sup> Incubation of Hck with ATP under conditions that led to stoichiometric phosphorylation of the activation loop tyrosine resulted in surprisingly subtle changes in deuterium uptake into the overall structure. In particular, ATP preincubation did not impact the interaction of the SH3 and SH2 domains with their respective internal ligands. This is consistent with previous biological and biochemical data suggesting that regulatory domain displacement is not necessary for kinase domain activation.<sup>7,23,33</sup> However, HX MS studies revealed that several Hck regions are highly dynamic, demonstrating maximum deuterium exchange at the earliest time point sampled (10 s). This was particularly true for peptides derived from the activation loop, which includes the autophosphorylation site (Tyr416). The implication is that this region of the kinase domain is continuously sampling the local environment, exposing Tyr416 for possible trans-phosphorylation by other kinases.

We next examined overall changes in Hck dynamics following incubation with the Nef protein of HIV-1. Hck is expressed primarily in macrophages, an important host cell for HIV-1, and interaction with Nef leads to constitutive Hck activation that may be important for enhancement of viral replication as well as immune escape. Remarkably, preincubation of Hck with Nef under conditions well-known to induce kinase activation produced surprisingly subtle changes in Hck dynamics. No net changes were observed in SH3 domain deuterium uptake, consistent with displacement of the SH2-kinase linker in response to Nef binding. Similarly, no changes were observed in SH2 peptides previously shown to be sensitive to changes in ligand binding, suggesting that interaction of Nef with Hck does not impact tail–SH2 interaction. This finding is consistent with earlier studies showing that activation of Hck by Nef in a cell-based assay did not impact regulatory tail tyrosine phosphorylation or require release from the SH2 domain.<sup>23</sup>

The magnitude of the changes in deuterium uptake observed in response to Nef binding were relatively modest, on the order of a few daltons. Therefore, arguments could be made that not all Hck-YEEI molecules in the population were bound, and that multiple populations of Hck-YEEI proteins (some bound, some free) coexist during labeling. As a consequence, the presence of mixed Hck-YEEI populations could be argued to complicate interpretation by obscuring subtle changes which did not rise above the error of the measurements. Two lines of evidence argue strongly against these concerns. First, we do not believe that only a small fraction of the Hck-YEEI population was bound by Nef in our studies. Based on our calculations, more than 95% of the Hck-YEEI proteins were bound to Nef, yet only small, highly localized changes in Hck-YEEI HX MS were observed. These small changes were on par with the small changes observed upon Hck-YEEI autophosphorylation, an event involving no other protein binding, no calculations of extent of interaction, and verified by phosphopeptide mapping as being over 98% complete. Even if, for sake of argument, most of the Hck-YEEI population of molecules was an unbound species, HX MS data interpretation would not be affected. The

HX MS technique is applied in a relative and comparative way, and the difference in regional deuterium uptake between two states is what is important (e.g., Hck-YEEI either alone or in the presence of Nef). As long as the representation of a complex in the population is large enough to be detected, then meaningful conclusions about the positions of the Nef-induced changes to the kinase can be made. While the magnitude of differences in deuterium level between bound and free is of interest, it is not paramount to making the determination as to which regions are affected by binding. Prior HX MS studies of SH3 domains in complex with peptide ligands help to illustrate this point. For example, deuterium exchange reactions in some cases were performed with 65% of the SH3 domains in the bound state due to limits of peptide solubility, yet local changes in SH3 domain HX that resulted from peptide binding were readily observed. For a comprehensive treatment of this topic, please see a recent review from Engen et al.<sup>34</sup>

In our measurements of Hck-YEEI bound to Nef, small changes were observed in three peptic peptides derived from the N-lobe of the kinase domain. One of these peptides, 247–267, encompasses the distal end of the SH2-linker as it joins the kinase domain N-lobe. This peptide also includes Trp260, which has been previously shown to have a critical function coupling the regulatory SH3:linker interaction to the kinase domain.<sup>42</sup> Rapid enhancement of deuterium exchange in the Nef-bound state is consistent with allosteric coupling of SH3:linker displacement to kinase activation. Larger and sustained changes in deuterium uptake were observed for peptide 286–302, which includes the highly conserved kinase domain residue Lys295. In virtually all known active kinase domain structures, this lysine forms a salt bridge with a conserved glutamate residue from the N-lobe  $\alpha$ C-helix. This interaction is critical to conformational positioning of residues involved in ATP binding and catalytic function. Enhanced deuterium uptake in the peptide encompassing this key lysine may promote kinase activation. Note that simply incubating Hck with ATP in the absence of Nef did not influence this peptide, suggesting that this dynamic change is a unique effect of Nef binding. More broadly, these HX MS results are consistent with an active complex structure that requires only modest changes in the SH3-linker interaction, such as the one modeled in Figure 2B.

Finally, we compared the effect of a unique small molecule inhibitor of Nef-induced Hck kinase activity (DFP-4AB) on deuterium uptake in the presence and absence of Nef. Preincubation of Hck-YEEI with this compound in the absence of Nef resulted in reduction of deuterium uptake into a peptide derived from the hinge region connecting the two kinase lobes, consistent with binding of this compound to the kinase domain active site. An X-ray crystal structure of Lck bound to a related DFP analog shows direct interactions with the hinge, supporting this view.<sup>39</sup> When this experiment was repeated in the presence of Nef, however, N-lobe peptide 286–302 became refractory to deuterium uptake in the presence of DFP-4AB, suggesting that this compound selectively inhibits the impact of Nef on this part of the active site (Figure 5).

The X-ray crystal structure of the kinase domain of Lck, another Src-family member and close relative of Hck, has been reported in complex with a very similar DFP-based inhibitor.<sup>39</sup> In this structure, the inhibitor-bound kinase domain adopts several hallmarks of the active state: the Lys:Glu salt bridge is present and the “DFG motif” is flipped inward. This structure suggests that Nef binding may induce the Hck kinase domain



to adopt a closely related conformation that in turn favors inhibitor binding. However, a formal “proof” of this mechanism will require an X-ray crystal structure of the Nef:Hck complex in the presence of DFP-4AB, which is the subject of ongoing investigation by our group.

Work presented here is consistent with a previous study showing an allosteric effect of Nef binding on the Hck active site.<sup>22</sup> This prior work used an engineered version of Hck with a modified SH3 domain that bound tightly to Nef as a way to maintain complex formation in solution kinase assays. In addition, the active site incorporated a “gatekeeper” point mutation that allowed for selective inhibition with the pyrazolopyrimidine compound, NaPP1. Using this system, Nef binding to the SH3 domain was shown to impact the Hck  $K_m$  for ATP as well as sensitivity to inhibition by NaPP1. These findings are consistent with our observations presented here that Nef binding impacts local dynamics near the Hck active site and that these changes are reversed in the presence of a selective inhibitor of the Nef:Hck complex.

## ■ ASSOCIATED CONTENT

### ■ Supporting Information

The Supporting Information is available free of charge on the ACS Publications website at DOI: 10.1021/acs.biochem.5b00875.

Table S1 and Supplementary Figures S1–S7 (PDF)

## ■ AUTHOR INFORMATION

### Corresponding Author

\*Northeastern University, 360 Huntington Ave., Boston, MA 02115-5000. E-mail: j.engen@neu.edu.

### Present Addresses

§J.M.H.: Sandia National Laboratory, PO Box 5800, Albuquerque, NM 87185.

||C.R.M.: Genzyme Corporation, 1 Mountain Rd., PO Box 9322, Framingham, MA 01701.

### Funding

This work was supported in part by National Institutes of Health Grants AI057083 and AI102724 (to T.E.S.), and GM086507 and GM101135 (to J.R.E.). HX MS support was provided through a research collaboration with the Waters Corporation (J.R.E.).

### Notes

The authors declare the following competing financial interest(s): JRE is a consultant of the Waters Corporation.

## ■ ACKNOWLEDGMENTS

The authors thank J.-J. Alvarado, University of Pittsburgh, for creating the models of the Nef:Hck-YEEI complex shown in Figure 2B,C and for critical reading of the manuscript.

## ■ REFERENCES

- (1) Guet, R.; Poincloux, R.; Castandet, J.; Marois, L.; Labrousse, A.; Le Cabec, V.; and Maridonneau-Parini, I. (2008) Hematopoietic cell kinase (Hck) isoforms and phagocyte duties - from signaling and actin reorganization to migration and phagocytosis. *Eur. J. Cell Biol.* 87, 527–542.
- (2) Pene-Dumitrescu, T., and Smithgall, T. E. (2010) Expression of a Src family kinase in chronic myelogenous leukemia cells induces resistance to imatinib in a kinase-dependent manner. *J. Biol. Chem.* 285, 21446–21457.

- (3) Pene-Dumitrescu, T.; Peterson, L. F.; Donato, N. J.; and Smithgall, T. E. (2008) An inhibitor-resistant mutant of Hck protects CML cells against the antiproliferative and apoptotic effects of the broad-spectrum Src family kinase inhibitor A-419259. *Oncogene* 27, 7055–7069.
- (4) Meyn, M. A., III; Wilson, M. B.; Abdi, F. A.; Fahey, N.; Schiavone, A. P.; Wu, J.; Hochrein, J. M.; Engen, J. R.; and Smithgall, T. E. (2006) Src family kinases phosphorylate the Bcr-Abl SH3-SH2 region and modulate Bcr-Abl transforming activity. *J. Biol. Chem.* 281, 30907–30916.
- (5) Saito, Y.; Yuki, H.; Kuratani, M.; Hashizume, Y.; Takagi, S.; Honma, T.; Tanaka, A.; Shirouzu, M.; Mikuni, J.; Handa, N.; Ogahara, I.; Sone, A.; Najima, Y.; Tomabechi, Y.; Wakiyama, M.; Uchida, N.; Tomizawa-Murasawa, M.; Kaneko, A.; Tanaka, S.; Suzuki, N.; Kajita, H.; Aoki, Y.; Ohara, O.; Shultz, L. D.; Fukami, T.; Goto, T.; Taniguchi, S.; Yokoyama, S.; and Ishikawa, F. (2013) A pyrrolo-pyrimidine derivative targets human primary AML stem cells in vivo. *Sci. Transl. Med.* 5, 181ra52.
- (6) Briggs, S. D.; Sharkey, M.; Stevenson, M.; and Smithgall, T. E. (1997) SH3-mediated Hck tyrosine kinase activation and fibroblast transformation by the Nef protein of HIV-1. *J. Biol. Chem.* 272, 17899–17902.
- (7) Moarefi, I.; LaFevre-Bernt, M.; Sicheri, F.; Huse, M.; Lee, C.-H.; Kuriyan, J.; and Miller, W. T. (1997) Activation of the Src-family tyrosine kinase Hck by SH3 domain displacement. *Nature* 385, 650–653.
- (8) Saksela, K. (2011) Interactions of the HIV/SIV pathogenicity factor Nef with SH3 domain-containing host cell proteins. *Curr. HIV Res.* 9, 531–542.
- (9) Malim, M. H., and Emerman, M. (2008) HIV-1 accessory proteins—ensuring viral survival in a hostile environment. *Cell Host Microbe* 3, 388–398.
- (10) Emert-Sedlak, L.; Kodama, T.; Lerner, E. C.; Dai, W.; Foster, C.; Day, B. W.; Lazo, J. S.; and Smithgall, T. E. (2009) Chemical library screens targeting an HIV-1 accessory factor/host cell kinase complex identify novel antiretroviral compounds. *ACS Chem. Biol.* 4, 939–947.
- (11) Narute, P. S., and Smithgall, T. E. (2012) Nef alleles from all major HIV-1 clades activate Src-family kinases and enhance HIV-1 replication in an inhibitor-sensitive manner. *PLoS One* 7, e32561.
- (12) Hung, C. H.; Thomas, L.; Ruby, C. E.; Atkins, K. M.; Morris, N. P.; Knight, Z. A.; Scholz, I.; Barklis, E.; Weinberg, A. D.; Shokat, K. M.; and Thomas, G. (2007) HIV-1 Nef assembles a Src family kinase-ZAP-70/Syk-PI3K cascade to downregulate cell-surface MHC-I. *Cell Host Microbe* 1, 121–133.
- (13) Dikeakos, J. D.; Atkins, K. M.; Thomas, L.; Emert-Sedlak, L.; Byeon, I. J.; Jung, J.; Ahn, J.; Wortman, M. D.; Kukull, B.; Saito, M.; Koizumi, H.; Williamson, D. M.; Hiyoshi, M.; Barklis, E.; Takiguchi, M.; Suzu, S.; Gronenborn, A. M.; Smithgall, T. E.; and Thomas, G. (2010) Small molecule inhibition of HIV-1-induced MHC-I down-regulation identifies a temporally regulated switch in Nef action. *Mol. Biol. Cell* 21, 3279–3292.
- (14) Smithgall, T. E., and Thomas, G. (2013) Small molecule inhibitors of the HIV-1 virulence factor, Nef. *Drug Discovery Today: Technol.* 10, e523–e529.
- (15) Emert-Sedlak, L. A.; Narute, P.; Shu, S. T.; Poe, J. A.; Shi, H.; Yanamala, N.; Alvarado, J. J.; Lazo, J. S.; Yeh, J. I.; Johnston, P. A.; and Smithgall, T. E. (2013) Effector Kinase Coupling Enables High-Throughput Screens for Direct HIV-1 Nef Antagonists with Antiretroviral Activity. *Chem. Biol.* 20, 82–91.
- (16) Tribble, R. P.; Narute, P.; Emert-Sedlak, L. A.; Alvarado, J. J.; Atkins, K.; Thomas, L.; Kodama, T.; Yanamala, N.; Korotchenko, V.; Day, B. W.; Thomas, G.; and Smithgall, T. E. (2013) Discovery of a diaminoquinoxaline benzenesulfonamide antagonist of HIV-1 Nef function using a yeast-based phenotypic screen. *Retrovirology* 10, 135.
- (17) Schindler, T.; Sicheri, F.; Pico, A.; Gazit, A.; Levitzki, A.; and Kuriyan, J. (1999) Crystal structure of Hck in complex with a Src family-selective tyrosine kinase inhibitor. *Mol. Cell* 3, 639–648.
- (18) Sicheri, F.; Moarefi, I.; and Kuriyan, J. (1997) Crystal structure of the Src family tyrosine kinase Hck. *Nature* 385, 602–609.

- (19) Xu, W., Doshi, A., Lei, M., Eck, M. J., and Harrison, S. C. (1999) Crystal structures of c-Src reveal features of its autoinhibitory mechanism. *Mol. Cell* 3, 629–638.
- (20) Xu, W., Harrison, S. C., and Eck, M. J. (1997) Three-dimensional structure of the tyrosine kinase c-Src. *Nature* 385, 595–602.
- (21) Chong, Y. P., Ia, K. K., Mulhern, T. D., and Cheng, H. C. (2005) Endogenous and synthetic inhibitors of the Src-family protein tyrosine kinases. *Biochim. Biophys. Acta, Proteins Proteomics* 1754, 210–220.
- (22) Pene-Dumitrescu, T., Shu, S. T., Wales, T. E., Alvarado, J. J., Shi, H., Narute, P., Moroco, J. A., Yeh, J. I., Engen, J. R., and Smithgall, T. E. (2012) HIV-1 Nef interaction influences the ATP-binding site of the Src-family kinase, Hck. *BMC Chem. Biol.* 12, 1.
- (23) Lerner, E. C., and Smithgall, T. E. (2002) SH3-dependent stimulation of Src-family kinase autophosphorylation without tail release from the SH2 domain in vivo. *Nat. Struct. Biol.* 9, 365–369.
- (24) Alvarado, J. J., Tarafdar, S., Yeh, J. I., and Smithgall, T. E. (2014) Interaction with the Src homology (SH3-SH2) region of the Src-family kinase Hck structures the HIV-1 Nef dimer for kinase activation and effector recruitment. *J. Biol. Chem.* 289, 28539–28553.
- (25) Triple, R. P., Emert-Sedlak, L., and Smithgall, T. E. (2006) HIV-1 Nef selectively activates SRC family kinases HCK, LYN, and c-SRC through direct SH3 domain interaction. *J. Biol. Chem.* 281, 27029–27038.
- (26) Moroco, J. A., Craigo, J. K., Iacob, R. E., Wales, T. E., Engen, J. R., and Smithgall, T. E. (2014) Differential sensitivity of Src-family kinases to activation by SH3 domain displacement. *PLoS One* 9, e105629.
- (27) Hochrein, J. M., Wales, T. E., Lerner, E. C., Schiavone, A. P., Smithgall, T. E., and Engen, J. R. (2006) Conformational features of the full-length HIV and SIV Nef proteins determined by mass spectrometry. *Biochemistry* 45, 7733–7739.
- (28) Engen, J. R. (1999) *Analysis of unfolding and protein dynamics in the regulatory domains of hematopoietic cell kinase with hydrogen exchange and mass spectrometry*. Ph.D. Thesis, University of Nebraska-Lincoln, Lincoln, NE.
- (29) Wales, T. E., Fadgen, K. E., Gerhardt, G. C., and Engen, J. R. (2008) High-speed and high-resolution UPLC separation at zero degrees Celsius. *Anal. Chem.* 80, 6815–6820.
- (30) Wang, L., Pan, H., and Smith, D. L. (2002) Hydrogen exchange-mass spectrometry: optimization of digestion conditions. *Mol. Cell. Proteomics* 1, 132–138.
- (31) Weis, D. D., Engen, J. R., and Kass, I. J. (2006) Semi-automated data processing of hydrogen exchange mass spectra using HX-Express. *J. Am. Soc. Mass Spectrom.* 17, 1700–1703.
- (32) Zhang, Z., and Smith, D. L. (1993) Determination of amide hydrogen exchange by mass spectrometry: a new tool for protein structure elucidation. *Protein Sci.* 2, 522–531.
- (33) Porter, M., Schindler, T., Kuriyan, J., and Miller, W. T. (2000) Reciprocal regulation of Hck activity by phosphorylation of Tyr(527) and Tyr(416). Effect of introducing a high affinity intramolecular SH2 ligand. *J. Biol. Chem.* 275, 2721–2726.
- (34) Engen, J. R., Wales, T. E., Chen, S., Marzluff, E. M., Hassell, K. M., Weis, D. D., and Smithgall, T. E. (2013) Partial cooperative unfolding in proteins as observed by hydrogen exchange mass spectrometry. *Int. Rev. Phys. Chem.* 32, 96–127.
- (35) Lerner, E. C., Triple, R. P., Schiavone, A. P., Hochrein, J. M., Engen, J. R., and Smithgall, T. E. (2005) Activation of the Src Family Kinase Hck without SH3-Linker Release. *J. Biol. Chem.* 280, 40832–40837.
- (36) Engen, J. R., Gmeiner, W. H., Smithgall, T. E., and Smith, D. L. (1999) Hydrogen exchange shows peptide binding stabilizes motions in Hck SH2. *Biochemistry* 38, 8926–8935.
- (37) Hochrein, J. M., Lerner, E. C., Schiavone, A. P., Smithgall, T. E., and Engen, J. R. (2006) An examination of dynamics crosstalk between SH2 and SH3 domains by hydrogen/deuterium exchange and mass spectrometry. *Protein Sci.* 15, 65–73.
- (38) Alvarado, J. J., Betts, L., Moroco, J. A., Smithgall, T. E., and Yeh, J. I. (2010) Crystal structure of the Src-family kinase Hck SH3-SH2-linker regulatory region supports an SH3-dominant activation mechanism. *J. Biol. Chem.* 285, 35455–35461.
- (39) Martin, M. W., Newcomb, J., Nunes, J. J., Bemis, J. E., McGowan, D. C., White, R. D., Buchanan, J. L., Dimauro, E. F., Boucher, C., Faust, T., Hsieh, F., Huang, X., Lee, J. H., Schneider, S., Turci, S. M., and Zhu, X. (2007) Discovery of novel 2,3-diarylfuro[2,3-b]pyridin-4-amines as potent and selective inhibitors of Lck: synthesis, SAR, and pharmacokinetic properties. *Bioorg. Med. Chem. Lett.* 17, 2299–2304.
- (40) Iacob, R. E., and Engen, J. R. (2012) Hydrogen exchange mass spectrometry: are we out of the quicksand? *J. Am. Soc. Mass Spectrom.* 23, 1003–1010.
- (41) Yamaguchi, H., and Hendrickson, W. A. (1996) Structural basis for activation of human lymphocyte kinase Lck upon tyrosine phosphorylation. *Nature* 384, 484–489.
- (42) LaFevre-Bernt, M., Sicheri, F., Pico, A., Porter, M., Kuriyan, J., and Miller, W. T. (1998) Intramolecular regulatory interactions in the Src family kinase Hck probed by mutagenesis of a conserved tryptophan residue. *J. Biol. Chem.* 273, 32129–32134.